

OPEN

Interplay between integrins and PI4P5K Sktl is crucial for cell polarization and reepithelialisation during *Drosophila* wound healing

Si-Hyoung Park^{1,2}, Chan-wool Lee^{1,2} & Kwang-Min Choe^{1*}

Phosphatidylinositol(4,5)-bisphosphate [PI(4,5)P₂] regulates cell adhesion and actin dynamics during cell migration. PI(4,5)P₂ binds various components of the cell adhesion machinery, but how these processes affect migration of the epithelial cell sheet is not well understood. Here, we report that PI(4,5)P₂ and Sktl, the kinase that converts PI4P to PI(4,5)P₂, are both localized to the rear side of cells during wound healing of the *Drosophila* larval epidermis. The Sktl localization requires JNK pathway activation and integrins, but not PVR. The *sktl* knockdown epidermis displays strong defects in wound closure, reminiscent of the JNK-depleted epidermis, and shows severe disruption of cell polarity, as determined by myosin II localization. Sktl and β PS integrin colocalize at the rear side of cells forming the trailing edge during wound healing and the two are inter-dependent in that the absence of one severely disrupts the rear localization of the other. These results strongly suggest that the JNK pathway regulates the rear localization of Sktl and integrins and the interplay between Sktl and integrins sets up cell polarity, which is crucial for reepithelialisation during wound healing.

Cell migration occurs through coordinated actions of polarization, protrusion, frontal adhesion, and detachment and retraction of the rear. Components involved in cell adhesion and migration are tightly regulated in a spatio-temporal manner, and the localization of specific molecules to the front or rear side of the cell is one of the most crucial aspects in cell migration because this sets up cell polarity and directionality^{1–3}.

Among the regulators that affect the behaviour of the cell migration machinery is phosphatidylinositol(4,5)-bisphosphate [PI(4,5)P₂]. PI(4,5)P₂ is present in the plasma membrane at relatively high concentrations, compared to other phosphoinositides⁴, and is synthesized from PI4P or PI5P by type I or type II phosphatidylinositol phosphate kinases (PIPKs), respectively, or from PI(3,4,5)P₃ by PTEN^{5,6}. PI(4,5)P₂ binds many cell adhesion proteins, including talin and vinculin, and also regulates the actin cytoskeleton by directly binding central actin-binding proteins^{7–13}. Most knowledge, however, was obtained in the context of single cell migration, and the possible interplay between PI(4,5)P₂, cell adhesion proteins, and their localization in cell-sheet migration has not been investigated well.

Wound healing is mediated by various cellular behaviours of multiple tissue types, but one of the most prominent features is reepithelialisation of cell sheets that cover wound holes^{14–16}. Wound healing of the *Drosophila* larval epidermis is an excellent model system to address the molecular mechanisms of cell-sheet migration, because wound healing in this system only involves cell growth and migration, but not proliferation¹⁷. In the *Drosophila* larva, reepithelialisation of a large wound hole is mediated by at least three different signalling pathways, JNK, PVR, and the Hippo pathways^{18–20}. Cell polarization and directionality are set up by a series of small GTPases, Cdc42, Rac1, and Rho1, which collectively mediate the wound signal to JNK and assemble myosin II at the wound margin and at the rear side of individual cells, which is clearly visible in cells that are located in the first three rows from the margin^{21–24}. Thus, the rear localization of myosin II is a convenient marker to assess cell polarization.

Integrins are heterodimeric membrane proteins, functioning as a cellular receptor in cell adhesion to the matrix. Integrins have a crucial role in cell migration and consequently in wound healing²⁵. In migrating single cells, integrins are often localized to the front side, while being degraded at the rear, which allows the uropod to detach from the matrix. Interestingly, we observed in *Drosophila* larva that α PS2- β PS integrin was localized to the rear side of

¹Department of Systems Biology, Yonsei University, 50 Yonsei-ro, Seodaemun-gu, Seoul, 03722, South Korea. ²These authors contributed equally: Si-Hyoung Park and Chan-wool Lee. *email: kmchoe@yonsei.ac.kr

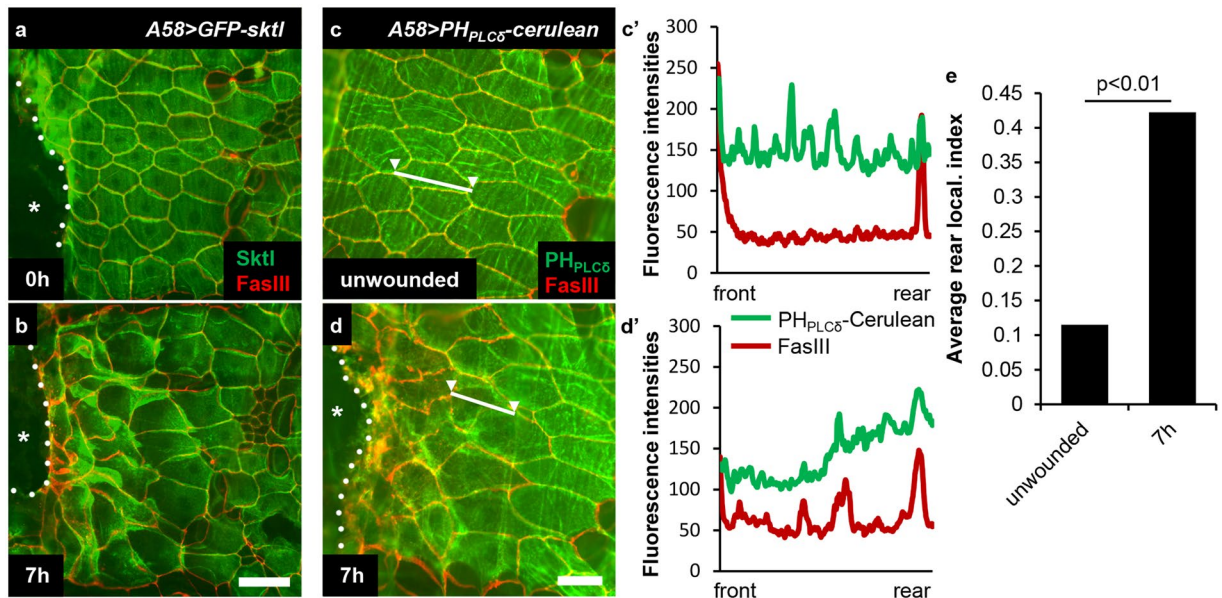


Figure 1. GFP-Sktl and PI(4,5)P₂ translocated to the rear side of epidermal cells during wound healing. **(a,b)** Localization of GFP-Sktl fusion protein, shown in green, after injury. **(a)** 0 h after injury. **(b)** 7 h after injury. **(c,d')** Distribution of PI(4,5)P₂, analysed using PH_{PLCδ}-Cerulean in unwounded **(c,c')** or wounded epidermis 7 h after injury **(d,d')**. **(c,d)** Epifluorescence of Cerulean from PH_{PLCδ}-Cerulean reporter in green. **(c',d')** Plotting of the fluorescence intensities along the frontal-rear axis of the cell in regard to the wound, marked with a white line with two arrowheads each in **(c,d)**. *A58-GAL4* is a larval epidermis-specific driver. *A58-GAL4 UAS-GFP-sktl* was abbreviated as *A58 > GFP-sktl*. Cell boundaries were stained with anti-FasIII antibody in red. The asterisk marks the wound hole and the white dotted line indicates the wound margin. Scale bars: 50 μm. **(e)** Rear localization index values for PH_{PLCδ}-Cerulean were calculated (see Methods). Mann–Whitney U-test was used for statistical significance.

cells during epidermal wound healing²⁶. Without αPS2-βPS and αPS3-βPS integrins, larvae displayed severe defects in wound closure^{26,27}. In mammalian cells, the integrin-containing adhesion complex is regulated by PI(4,5)P₂ during cell migration⁶. Specifically, talin binds to PI(4,5)P₂ via its FERM domain, which targets talin to focal adhesions, and increases affinity for β integrin when analysed in HeLa and NIH3T3 cells⁸. Vinculin binds PI(4,5)P₂ via its tail and this appears to promote disassembly of focal adhesions and cell migration of mouse melanoma cells¹¹. Whether these types of regulation occur *in vivo*, particularly during cell-sheet migration, has rarely been studied.

Here, we focused on Sktl in *Drosophila* wound healing. The *Drosophila* genome contains two genes that encode the phosphatidylinositol-4-phosphate 5-kinase (PIP5K), which are *sktl* and *dPIP5K*²⁸. *sktl* is involved in diverse processes, including vesicle trafficking, setting up apical-basal polarity²⁹, and ciliogenesis³⁰. *dPIP5K* is essential for re-synthesis of PIP₂ in photoreceptors²⁸. In the present study, we report that Sktl was localized to the rear side of epidermal cells in a JNK-dependent manner during wound healing. Sktl colocalized with integrins, and the interplay between the two was essential for setting up cell polarity and wound closure.

Results

GFP-Sktl and PI(4,5)P₂ translocate to the rear side of epidermal cells during wound healing.

To investigate possible roles of PI(4,5)P₂ in *Drosophila* wound healing, we analysed the localization of Sktl protein after epidermal injury generated by pinching the cuticle and abrading approximately 30 epidermal cells. Before or immediately after wounding, the functional fusion protein GFP-Sktl³¹ was evenly distributed in the dorsal epidermal cells of the third instar larva, but translocated to the rear side of the cell during wound healing, which was most evident in the first 2–3 rows of cells from the wound margin. The localization was noticeable 4 h after injury and became distinct by 7 h, the time interval when cells changed their shapes dramatically and migrated to close the wound hole (Fig. 1a,b)²¹. We analysed the endogenous Sktl protein and obtained similar results (see Fig. 2c). We also examined the localization of PI(4,5)P₂ using the reporter gene PH_{PLCδ}-Cerulean³². Although the distribution pattern was subtle, the plotting results of the fluorescence intensity of Cerulean across the frontal-rear axis of the cells indicated that the levels of PI(4,5)P₂ also increased on the rear side during wound healing (Fig. 1c–e; see Methods for the quantification of rear localization).

The rear localization of Sktl requires JNK and integrins, but not PVR. To identify the regulators for Sktl localization, we examined Sktl localization in different genetic backgrounds where the signalling pathways critical for wound closure were deficient. In the larval epidermis expressing the gene encoding a dominant negative form of the *Drosophila* JNK (*bsk^{DN}*), cells remained largely polygonal in shape after injury, as reported previously^{18,21}. GFP-Sktl was also evenly distributed across the cell, which was in drastic contrast to wild type (Fig. 2a,b'). We quantified the rear localization of GFP-Sktl based on the GFP fluorescence intensity (Fig. 2c). In

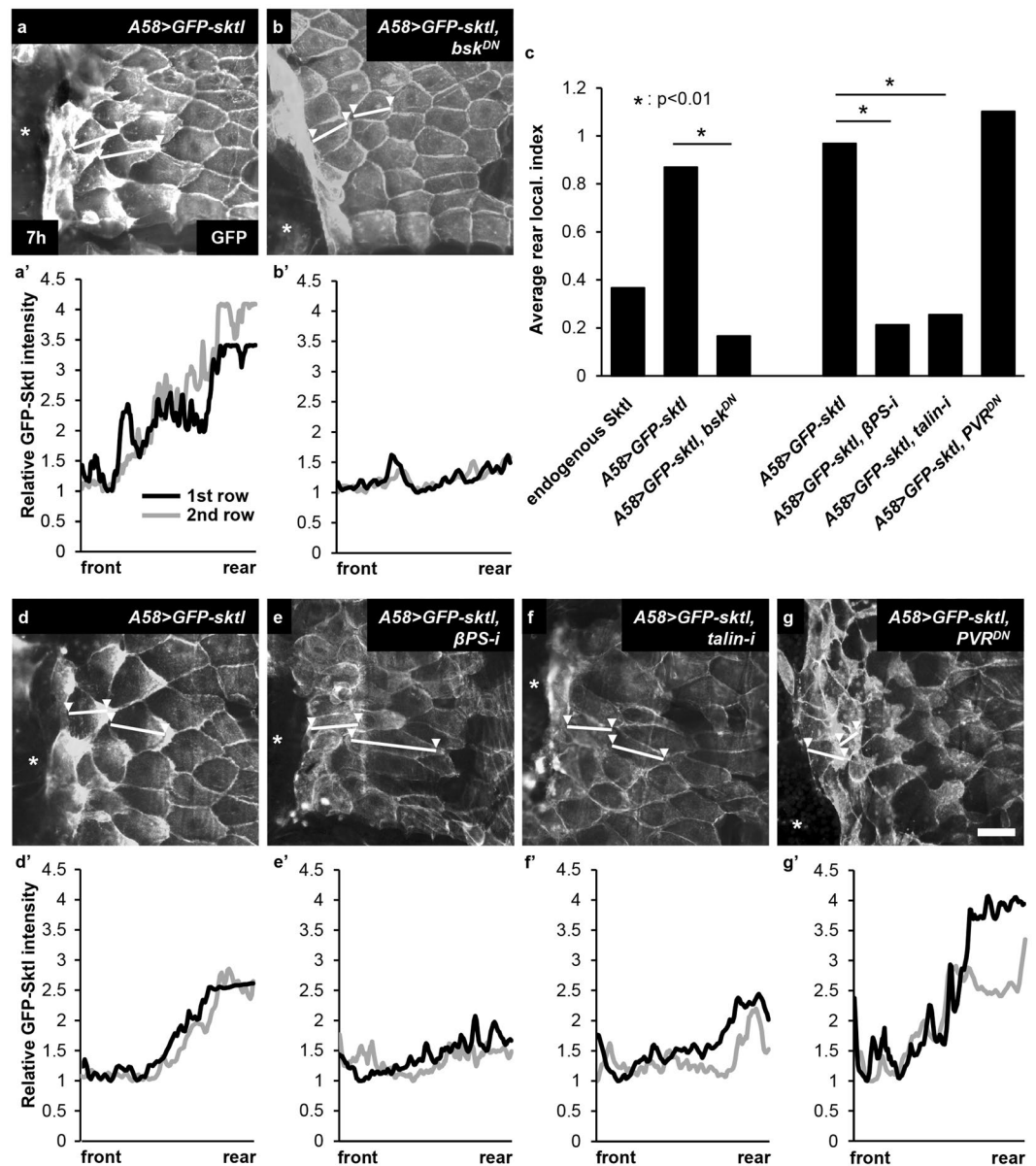


Figure 2. Sctl localization required JNK and integrins, but not PVR. Sctl localization was analysed in the larval epidermis expressing GFP-Sctl, shown in white, 7 h after wounding. (**a,d**) Controls. (**b**) $A58 > bsk^{DN}$. (**c**) Quantification of the rear localization of GFP-Sctl in the first two rows of cells, presented with the rear localization index value (see Methods for calculation). (**e**) $A58 > \beta PS-RNAi$. ($A58 > \beta PS-i$, hereafter). (**f**) $A58 > talin-i$. (**g**) $A58 > PVR^{DN}$. The asterisk indicates the wound hole. (**a',b',d'-g'**) Plotting of the GFP fluorescence intensities along the frontal-rear axis of the cells in the 1st row (black) and the 2nd row (grey) from the wound margin. The axes were marked in white lines with two arrowheads in (**a,b,d-g**). Scale bar: 50 μ m. For statistical analysis, Mann-Whitney U-test was used.

the larval epidermis expressing RNAi for integrin βPS (*mys*) or *taln* (*rhea*), cells changed their shapes moderately, consistent with the delayed closure of the wound hole²⁶, but the rear localization of GFP-Sctl was severely disrupted (Fig. 2c,d-f'). In the larval epidermis expressing the gene encoding a dominant negative form of PVR (PVR^{DN}), GFP-Sctl translocated to the rear side, which was essentially the same as in wild-type (Fig. 2c,g,g'). Altogether, we conclude that Sctl localization requires JNK and integrins, but not PVR.

***sktl* is required for wound closure.** We examined whether *sktl*-deficient larvae displayed wound closure defects. Because the null mutations of *sktl* are embryonic lethal^{31,33}, we knocked down the gene via *UAS-RNAi* transgenes using the larval epidermis-specific $A58-GAL4^{18}$. *sktl* knockdown using two independent RNAi lines targeting different regions of *sktl* equally and effectively blocked closure of a wound hole with the size of approximately 30 epidermal cells analysed 16 h after injury, whereas *GAL4*-only control larvae had completely closed the wound hole by that time (Fig. 3a-c,f). We confirmed the result by rescuing the open-wound phenotype

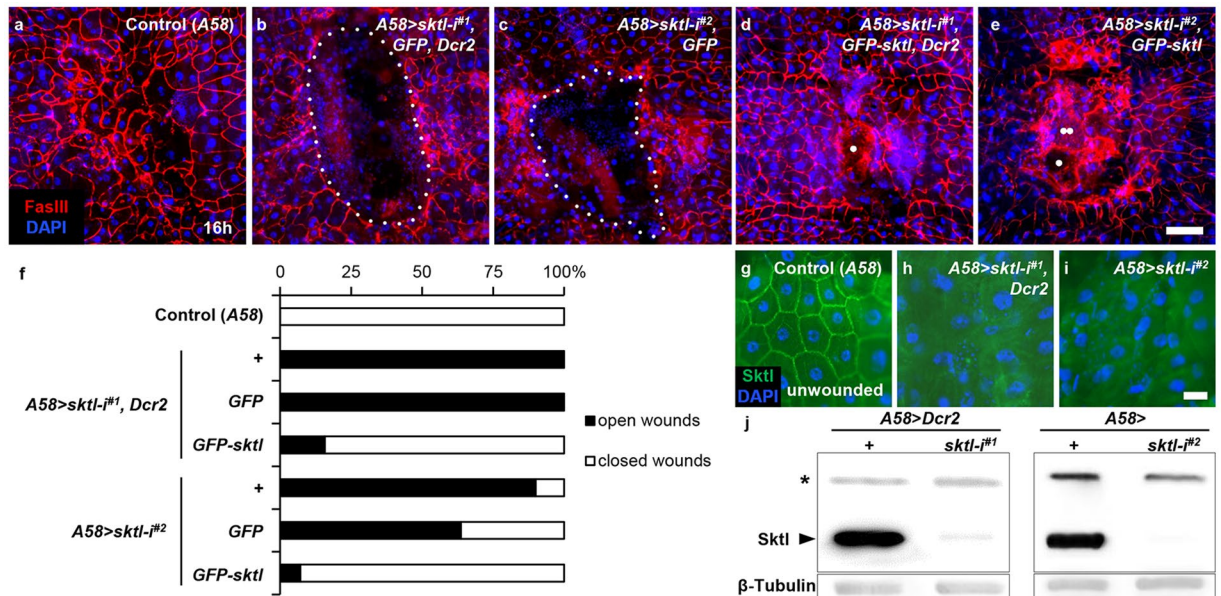


Figure 3. *sktl* was required for wound closure. Wound closure was analysed 16 h after wounding. (a) A58-only control. (b) A58 > *sktl-i^{#1}*, GFP, Dcr2. (c) A58 > *sktl-i^{#2}*, GFP. (d) A58 > *sktl-i^{#1}*, GFP-sktl, Dcr2. (e) A58 > *sktl-i^{#2}*, GFP-sktl. (f) Quantification of wound closure. UAS-GFP was added to balance the UAS copy number. Cell nuclei were stained with DAPI in blue and cell boundaries were stained with anti-FasIII antibodies in red. The white dotted line indicates an open-wound hole. The white single dots in (d,e) indicate scabs induced by breaches on the epidermal-cuticle layer during wounding. The white twin dots in (e) indicate large fused cell(s) that form occasionally during wound healing. For each genotype, at least 10 larvae were examined. (g–j) Confirmation of the knockdown efficiency in unwounded larval epidermis of the indicated genotypes by immunostaining (g–i) or Western blots (j) using anti-Sktl antibody. (g) A58-only control. (h) A58 > *sktl-i^{#1}*, Dcr2. (i) A58 > *sktl-i^{#2}*. Sktl protein was visualized using anti-Sktl antibody in green, and the cell nuclei were stained with DAPI in blue. In Western blotting, β -Tubulin was used as a loading control. The asterisk indicates a non-specific band (see Supplemental Fig. S3 for full-length blots). Scale bar: 100 μ m (a–e); 25 μ m (g–i).

by simultaneously overexpressing UAS-GFP-*sktl* (Fig. 3d–f; UAS-GFP was added to control groups to balance the UAS copy number). We also confirmed that in *sktl*-knockdown larval epidermis, Sktl protein was substantially reduced, as examined by anti-Sktl antibody staining and Western blotting (Fig. 3g–j; Supplemental Fig. 3). Altogether, *sktl* is required for larval epidermal wound closure.

The *sktl* requirement might be ascribed, not to the function of PI(4,5)P2 itself, but to PI(4,5)P2 serving as a precursor for the synthesis of PI(3,4,5)P3, so far, the most versatile and dynamically regulated type of phosphoinositides^{6,13}. Alternatively, it might be due to the requirement for diacylglycerol (DAG) and inositol 1,4,5 triphosphate (IP3), which are generated by the hydrolysis of PI(4,5)P2 by phospholipase C (PLC). We examined wound closure in various larvae where the activities of the key enzymes catalysing each of these reactions were depleted and found that the wound holes closed normally when examined at 16 h (Supplemental Fig. S1). Thus, we conclude the *sktl* requirement for wound closure is not due to a lack of PI(3,4,5)P3, DAG, or IP3.

***sktl* knockdown larvae display disrupted cell polarization during wound healing.** We examined further Sktl function in cell polarization during wound healing via the localization of nonmuscle myosin II^{21,22}. In wild-type, the myosin II heavy chain Zip and the functional fusion protein GFP-Zip translocate to the rear side of cells 4–8 h after injury, which requires JNK pathway activation²¹.

In wild-type larvae, 89.1% of the cells located in the first two rows from the wound margin responded correctly to the wound stimulus, as measured by GFP-Zip translocation 7 h after injury (Fig. 4a,c). In *sktl* knockdown larvae, in contrast, merely 11.8% of the cells located within the same distance responded correctly ($p < 0.01$), and the rest of the cells failed to relocate GFP-Zip; the protein remained mainly in the peri-nuclear region as if the cells did not receive the wound signals (Fig. 4b,c). The cells displaying the wrong directionality were very minor; 5.4% in wild-type and 3.9% in *sktl* knockdown larvae (Fig. 4c).

For epistatic analysis, we performed the reverse experiments, analysing the localization of GFP-Sktl protein in *zip* knockdown larvae. Knockdown of *zip* made larval epidermal cells slightly abnormal and unhealthy, as observed previously²¹, and consequently, the localization pattern of GFP-Sktl was not as distinct as in wild-type. Nonetheless, the rear localization of GFP-Sktl protein was observed in many of the first three rows of cells (Fig. 4d,e). Thus, Sktl, and possibly PI(4,5)P2, are critically involved in setting up cell polarity during wound healing and functions upstream of myosin II.

We also examined whether JNK pathway activation was affected by Sktl depletion. Induction of the JNK pathway reporter *msn-lacZ*, analysed 7 h after wounding, was grossly normal in *sktl* knockdown larval epidermis (Supplemental Fig. 2). Therefore, we concluded that Sktl functions downstream of JNK and upstream of myosin II during wound closure.

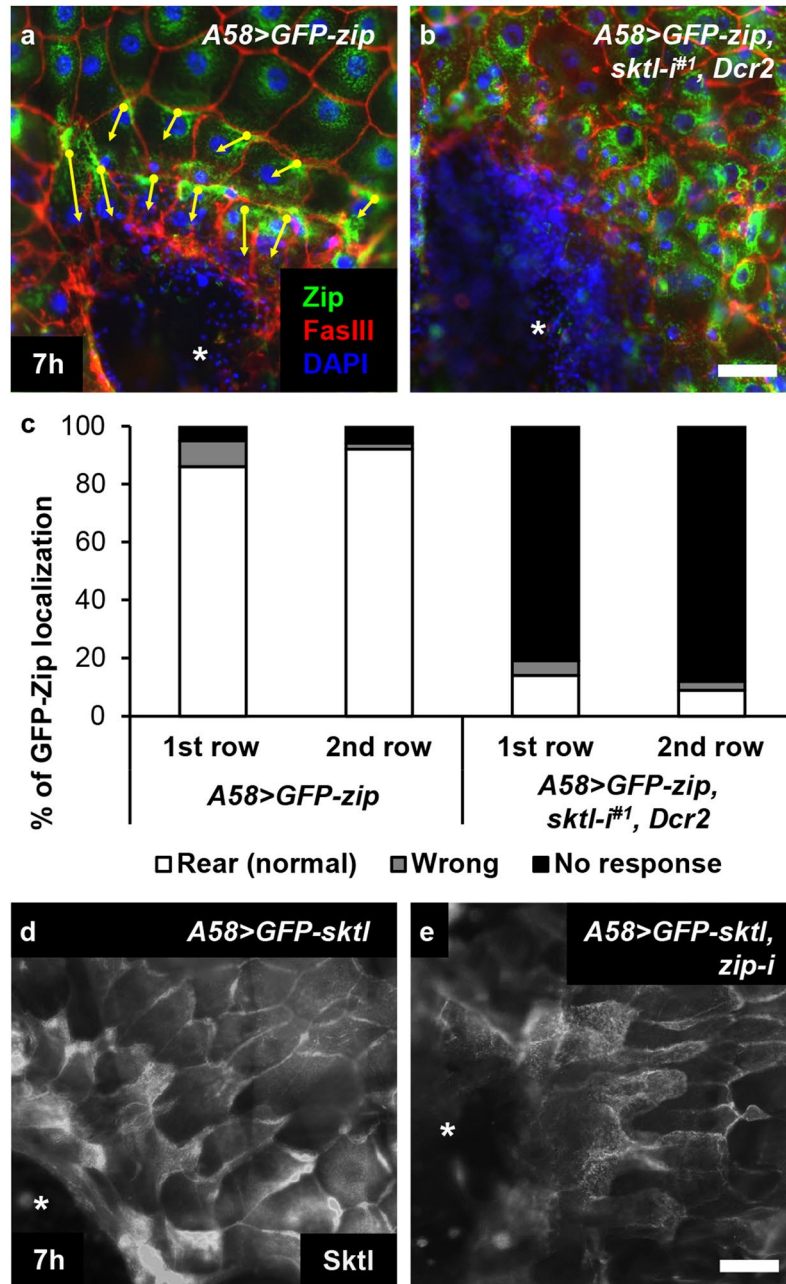


Figure 4. *sktl* was required for the rear localization of myosin II during wound healing. (a,b) Localization of nonmuscle myosin II was analysed via GFP-Zip in green 7h after wounding. (a) *A58 > GFP-zip*. (b) *A58 > GFP-zip, sktl-#1, Dcr2*. Cell nuclei were visualized by DAPI staining in blue and cell boundaries were visualized by anti-FasIII antibody staining in red. The arrows indicate directionality of the cells in the first two rows from the wound margin, based on GFP-Zip localization. (c) Quantification of the results in (a,b). The drastic reduction in the numbers of cells with normal polarization in *sktl*-knockdown larvae is statistically significant ($p < 0.01$). Mann–Whitney U-test was used. (d,e) The rear localization of GFP-Sktl protein, shown in white, was analysed in the larvae depleted of the myosin II heavy chain. (d) *A58 > GFP-sktl*. (e) *A58 > GFP-sktl, zip-i*. The asterisks indicate wound holes. Scale bars: 50 μ m.

***sktl* knockdown larvae are defective in rear localization of β PS integrin during wound healing.**

We also assessed cell polarization via immunostaining for β PS integrin, another protein that localizes at the rear side of cells during larval wound healing of the epidermis²⁶. In control larvae, β PS integrin localized to the rear side of the cells in the first two rows from the wound margin 7h after injury, as reported previously (Fig. 5a,a')²⁶. In *sktl* knockdown epidermis, however, β PS integrin appeared evenly distributed in most cells (Fig. 5b,b'). In *GFP-sktl*-expressing, knockdown-rescued epidermis, the localization pattern of β PS integrin was also rescued (Fig. 5c,c'). We quantified the results and calculated the rear localization index value (Fig. 5d). Together with the results in Fig. 2e,f we conclude that Sktl and β PS integrin are inter-dependent for their rear localization.

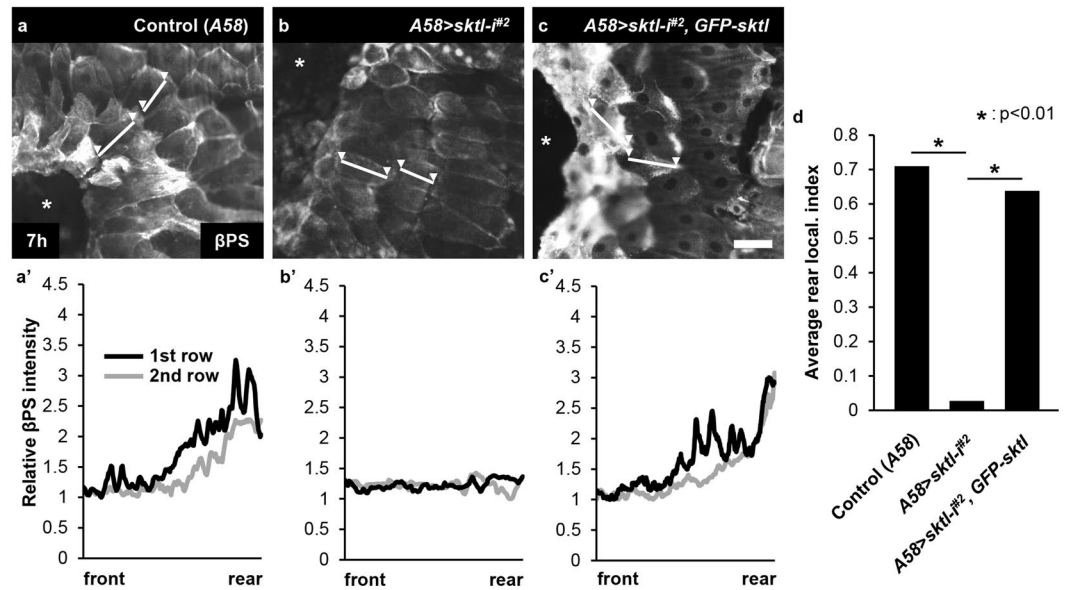


Figure 5. *sktl* was required for the rear localization of β PS integrin during wound healing. β PS localization was examined using anti- β PS antibody staining in white 7h after wounding. (a) A58-only control. (b) A58 > *sktl-i#2*. (c) A58 > *sktl-i#2*, GFP-*sktl*. The asterisks indicate wound holes. Scale bar: 50 μ m. (a'-c') Plotting of the fluorescence intensities along the frontal-rear axis of the cells in the 1st row (black) and the 2nd row (grey) from the wound margin. The axes were marked in white lines with two arrowheads in (a-c). (d) Quantification of the rear localization of β PS integrin in the first two rows of cells, presented with the rear localization index value. For statistical analysis, Mann-Whitney U-test was used.

Sktl and β PS integrin colocalize in the rear side of cells during wound healing. Because Sktl and β PS integrin both localized to the rear side of cells during wound closure, we directly analysed their colocalization in unwounded samples and wounded samples 7h after injury, the time point when their rear localization became most prominent (Fig. 1; data not shown)²⁶. First, β PS localized on the basal side of the epidermal cells facing the basement membrane, visualized using Vkg-GFP (Fig. 6a), and E-cad was on the lateral side, presumably marking the adherens junction (Fig. 6b,c)³⁴. In wounded epidermis, β PS integrin and Sktl colocalized to the rear part of cells that appeared the trailing edge (Fig. 6d,d'). E-cad protein was maintained laterally (Fig. 6d,e'), whereas the rear part of the cell overlapped with the front part of the cells in the next row, as if the cells lying behind crawled on the cells ahead (Fig. 6d,e'). Consistently, anti-E-cad staining and anti- β PS staining did not overlap in this region; anti-Sktl and anti- β PS staining visualized the presumptive trailing edge, whereas anti-E-cad staining tended to display pentagonal or hexagonal shapes of the cell (Fig. 6d,e'). Localization of FasIII, a septate junction protein that is more basally located, compared to E-cad (Fig. 6e') similarly marked polygonal shapes of cells (Fig. 6e,e'). Thus, in the rear part of the cell, the region demarcated by E-cad and β PS integrin seems to form the trailing edge, and this was the region with concentrated β PS integrin and Sktl (Fig. 6f).

Discussion

Here, we report that *sktl*, encoding a *Drosophila* PI4P5K, is required for wound closure of the larval epidermis. Sktl and β PS integrin help each other colocalize to the rear side of cells during wound healing, and this interaction is crucial for setting up cell polarity, which leads to the rear localization of myosin II and reepithelialisation.

We showed, here and previously, that JNK was upstream of these events, as depletion of JNK activation led to disruption of all the events^{21,26}. On the other hand, JNK pathway activation was normal in *sktl*, β PS, *talin*, or *zip* knockdown larvae. *sktl* or β PS knockdown larvae showed disruption in myosin II localization, but *zip* knockdown did not affect Sktl localization. Thus, wounding in the larval epidermis generates as-yet unknown signals that activate the Rho-family small GTPases²², which may be activated differentially in the front and the rear sides of the cell, similar to that in single cell migration^{2,3}; this leads to the activation of JNK²², which is translated to the rear localization of Sktl and β PS integrin²⁶.

An interesting question is then the mechanism of how JNK signalling relays the information of cell polarity. In a wounded field, JNK signalling is activated in a graded manner, waning towards the distal area, as analysed by the induction of *msn-lacZ* or *puc-lacZ*¹⁸. It is thus plausible that JNK itself provides the frontal-rear information in individual cells, based on the minute difference in JNK activation levels across the frontal-rear axis of individual cells, and possibly, via mutual inhibition between the front and the rear². Alternatively, it may be that a missing factor provides such information and JNK is merely an essential bystander.

We observed that both Sktl protein and PI(4,5)P2 localized to the rear side, but did not provide data to argue strongly that it is PI(4,5)P2 that executes setting up the cell polarity and possibly integrin regulation. One way to address this issue would be to carefully perturb PI(4,5)P2 levels or to swap the wild-type Sktl with a kinase-dead version. Sktl is involved in various processes including cell viability, cytoskeletal organization of actin and

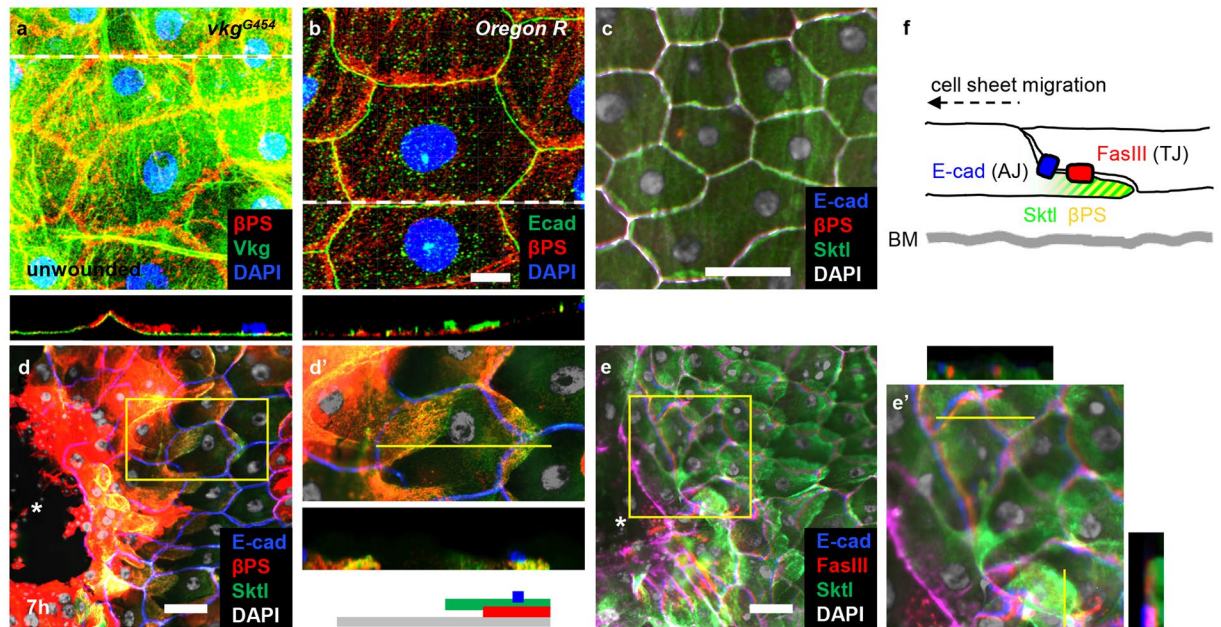


Figure 6. Sktl and β PS proteins colocalized to the rear side of cells during wound healing. Colocalization of Sktl and β PS was examined in un wounded condition (a–c) or 7h after wounding (d–e). (a) *vkg^{G454}*. (b–e) *Oregon R*. (d,e) High-magnification views of the areas marked in yellow boxes in (d,e). Collagen IV was visualized using the protein trap line *vkg^{G454}* in green (a). β PS was stained with anti- β PS antibody in red (a–d). E-cad was stained with anti-E-cad antibody in green (b) or blue (c–e). Sktl was stained with anti-Sktl antibody in green (c–e). Cell nuclei were stained with DAPI in blue (a,b) or white (c–e). The asterisks indicate wound holes (d,e). The grey line of the diagram under (d) indicates the length of a cell. The yellow lines in (d,e) indicate the positions of optical sectioning. (f) A proposed diagram showing the relative position of each component. AJ: adherens junctions; TJ: tight junctions; BM: basement membranes. Scale bar: 10 μ m (b); 50 μ m (c–e).

microtubule, and polar transport of mRNA, proteins, and vesicles^{31,33,35–37}, and the PI(4,5)P2 requirement was nicely shown in some of these cases^{35,36}. PI(4,5)P2 interacts with talin, vinculin, moesin, myosin-X, and factors involved in cytoskeletal reorganisation⁶. We, therefore, favour the hypothesis that Sktl and the integrin-containing adhesion complex interact with each other to localize to the rear, and the resulting increase of the local concentration of PI(4,5)P2 affects the behaviour of the adhesion complex and promotes epithelial wound closure.

Lastly, it is worth mentioning some unresolved questions in our study. The first is the question of how PI(4,5)P2 affects the integrin adhesion complex and ultimately reepithelialisation. Interaction between talin and PI4P5K or PI(4,5)P2^{38,39} enhances talin binding either to β integrin in mammalian mesenchymal cells^{6,8} or to myosin II in *Dictyostelium*⁴⁰. These results are, however, inconsistent with our observation that focal adhesion-like structures containing talin were not particularly enriched in the posterior of the cells during reepithelialisation (data not shown). Thus, the two systems must work differently, and a more careful investigation of the function of PI(4,5)P2 may be necessary. Second, our results showing that the presumptive trailing edge of the cells underlies the frontal part of the cells behind are intriguingly different from what has been observed in the migration of MDCK cell sheets, in which the forward protrusion of so-called cryptic lamellipodia of submarginal cells contributes to cell-sheet migration⁴¹. Future studies should explore the function of the rear localization of PI(4,5)P2, PI4P5K, and integrins, as regulation of PI4P5K activity might be intimately related to various diseases including cancer metastasis^{42–44}.

Methods

Fly strains. The following stocks were obtained from the Bloomington Stock Center: *msn-lacZ* (*msn*⁰⁶⁹⁴⁶; 11707), *UAS-sktl-RNAi* (27715), *UAS-bsk^{DN}* (6409), *UAS-PVR^{DN}* (58430), *UAS-GFP-nls* (4776), *UAS-Dcr2* (25706), *UAS-Pi3K92E^{A2860C}* (8289), and *UAS-Pten-RNAi* (8549, 8550). The following stocks were obtained from the Vienna *Drosophila* RNAi Center: *UAS-sktl-RNAi* (101624), *UAS-zip-RNAi* (7819), *UAS-norPA-i* (105676), *UAS-sl-i* (108593), and *UAS-PLC21C-i* (26558). The following stocks were obtained from the National Institute of Genetics: *UAS- β PS-RNAi* (1560R-1) and *UAS-talin-RNAi* (6831R-1). The following stocks were obtained from private lab collections: *A58-GAL4¹⁸*, *UAS-GFP-sktl³¹*, *UAS-PH_{PLC δ} -cerulean³²*, *UAS-GFP-zip⁴⁵*, *norPA^{P2446}*, and *vkg^{G454}*.

Wounding and immunohistochemistry. Third instar larvae were wounded on the dorsal side of segment A2 or A3 by gently pinching the epidermis/cuticle with a pair of forceps (Fine Science Tools, Cat. No. 11295-00). Larvae were incubated on cornmeal-agar media for wound healing. The larval epidermis was dissected in phosphate-buffered saline (PBS) and fixed in 4% paraformaldehyde for 15 min.

Fixed samples were washed three times in [PBS plus 0.5% Triton X-100 (PBST) supplemented with 5% normal goat serum (Gibco, Cat. No. 1913391)] (PBST-NGS) and pre-incubated with PBST-NGS for 1 h. Samples were then incubated with primary antibodies diluted in PBST-NGS overnight at 4 °C. The following primary antibodies were used: mouse anti-Fasciclin III [1:50 dilution; Developmental Studies Hybridoma Bank (DSHB), Cat. No. 7G10], mouse anti- β PS (1:50 dilution; DSHB, Cat. No. CF6G11), mouse anti- β -galactosidase (1:100 dilution; DSHB, Cat. No. JIE7), rat anti-E-cadherin (1:50 dilution; DSHB, Cat. No. DCAD2), and rabbit anti-Sktl (1:100 dilution)²⁹. Samples were washed in PBST-NGS three times for 10 min and incubated with secondary antibodies diluted in PBST overnight at 4 °C. The following secondary antibodies were used: Cy3-conjugated goat anti-mouse IgG (1:100; Jackson ImmunoResearch, Cat. No. 75512), Alexa 488-conjugated goat anti-mouse IgG (1:200; Molecular Probes, Cat. No. A11001), Alexa 488-conjugated goat anti-rabbit IgG (1:200; Molecular Probes, Cat. No. A11008), Alexa 488-conjugated goat anti-rat IgG (1:200; Molecular Probes, Cat. No. A11006), Alexa 546-conjugated goat anti-rabbit IgG (1:200; Molecular Probes, Cat. No. A11010), and Cy5-conjugated goat anti-mouse IgG (1:100; Jackson ImmunoResearch, Cat. No. 72032). After washing in PBST-NGS five times for 10 min each, samples were mounted on a slide glass using Vectashield (Vector Laboratories, Cat. No. H-1000) and subjected to fluorescence microscopy (ZEISS Axio Imager 2) or confocal microscopy (ZEISS LSM 880). Cell nuclei were stained with 4',6-diamidino-2-phenylindole (DAPI; Molecular Probes, Cat. No. D1306) at 1:500 dilution.

Quantification of the rear localization of PH_{PLC δ} -Cerulean, Sktl-GFP, Sktl, and β PS integrin.

The fluorescence intensity of Cerulean, GFP, or other fluorophores from immunohistochemical staining was measured along the frontal-rear axis of a marginal cell in the wounded area using ImageJ 2 A. Upon determining the frontal-rear axis, the longest line that lied within $\pm 45^\circ$ from the hypothetical perpendicular line towards the wound centre was chosen. The rear localization index was calculated as follows: (the intensity value of the rear half of the cell – that of the frontal half) divided by the intensity value of the frontal half. At least > 80% of the total cells located in the first and second rows from the wound margin were measured, which removed non-analysable cells due to damage or other abnormal conditions. At least six larvae were examined per genotype. For the case of PH_{PLC δ} -Cerulean, at least > 70% of the total cells located in the first and second rows from the wound margin were examined in four larvae.

Quantification of GFP-Zip localization. The localization of GFP-Zip was examined in the first two rows of cells from the wound margin. A line with an arrowhead was drawn in each of these cells by placing its arrowhead on the nucleus and the endpoint on the middle of GFP-Zip aggregation. If the arrow had a direction that was within $\pm 45^\circ$ from the hypothetical wounded centre, the cell was sorted as 'normal'. If the arrow was directing outside of the range, the cell was sorted as 'wrong'. If GFP-Zip remained as if the cell did not receive wound signals (similar to the cells in unwounded samples), the cell was sorted as 'no response'. At least 70% of the total cells located in the first and second rows from the wound margin were in analysable conditions, and eight larvae were examined.

Western blot analysis. Larval epidermal samples were boiled in sodium dodecyl sulfate (SDS) sample buffer [250 mM Tris-HCl (pH 6.8), 0.5 M dithiothreitol, 10% SDS, 0.25% bromophenol blue, and 50% glycerol] for 5 min, subjected to 10% SDS-polyacrylamide gel electrophoresis, and were transferred to nitrocellulose membranes. The membranes were blocked with 5% skim milk in TBST [10 mM Tris (pH 8.0), 150 mM NaCl, and 0.05% Tween 20] for 1 h, and probed with primary antibodies at 4 °C overnight. The following primary antibodies were used: rabbit anti-Sktl (1:500 dilution)²⁹, and goat anti- β -Tubulin (1:1000 dilution; Santa Cruz Biotechnology, Inc.). The membranes were washed three times in TBST and incubated with HRP-conjugated secondary antibodies [1:1000 dilution; anti-rabbit (Cat. No. sc-2004), and anti-goat (Cat. No. sc-2056)] in TBST with 1% skim milk for 1 h. After washing in TBST three times, the membranes were visualized using the WEST-ZOL Plus[®] Western blot detection system (iNtRon, Cat. No. 16024).

Received: 24 April 2019; Accepted: 22 October 2019;

Published online: 08 November 2019

References

- Li, Z. *et al.* Directional sensing requires G beta gamma-mediated PAK1 and PIX alpha-dependent activation of Cdc42. *Cell* **114**, 215–227 (2003).
- Meili, R. & Firtel, R. A. Two poles and a compass. *Cell* **114**, 153–156 (2003).
- Xu, J. *et al.* Divergent signals and cytoskeletal assemblies regulate self-organizing polarity in neutrophils. *Cell* **114**, 201–214 (2003).
- Lemmon, M. A. Membrane recognition by phospholipid-binding domains. *Nature reviews. Molecular cell biology* **9**, 99–111, <https://doi.org/10.1038/nrm2328> (2008).
- Yin, H. L. & Janmey, P. A. Phosphoinositide regulation of the actin cytoskeleton. *Annu Rev Physiol* **65**, 761–789, <https://doi.org/10.1146/annurev.physiol.65.092101.142517> (2003).
- Ling, K., Schill, N. J., Wagoner, M. P., Sun, Y. & Anderson, R. A. Movin' on up: the role of PtdIns(4,5)P(2) in cell migration. *Trends in cell biology* **16**, 276–284, <https://doi.org/10.1016/j.tcb.2006.03.007> (2006).
- DeMali, K. A., Barlow, C. A. & Burridge, K. Recruitment of the Arp2/3 complex to vinculin: coupling membrane protrusion to matrix adhesion. *J Cell Biol* **159**, 881–891, <https://doi.org/10.1083/jcb.200206043> (2002).
- Martel, V. *et al.* Conformation, localization, and integrin binding of talin depend on its interaction with phosphoinositides. *The Journal of biological chemistry* **276**, 21217–21227, <https://doi.org/10.1074/jbc.M102373200> (2001).
- Skare, P. & Karlsson, R. Evidence for two interaction regions for phosphatidylinositol(4,5)-bisphosphate on mammalian profilin I. *FEBS letters* **522**, 119–124 (2002).
- Lambrechts, A., Jonckheere, V., Dewitte, D., Vandekerckhove, J. & Ampe, C. Mutational analysis of human profilin I reveals a second PI(4,5)-P2 binding site neighbouring the poly(L-proline) binding site. *BMC Biochem* **3**, 12 (2002).
- Chandrasekar, I. *et al.* Vinculin acts as a sensor in lipid regulation of adhesion-site turnover. *Journal of cell science* **118**, 1461–1472, <https://doi.org/10.1242/jcs.01734> (2005).

12. Saarikangas, J., Zhao, H. & Lappalainen, P. Regulation of the actin cytoskeleton-plasma membrane interplay by phosphoinositides. *Physiol Rev* **90**, 259–289, <https://doi.org/10.1152/physrev.00036.2009> (2010).
13. Senju, Y. & Lappalainen, P. Regulation of actin dynamics by PI(4,5)P₂ in cell migration and endocytosis. *Current opinion in cell biology* **56**, 7–13, <https://doi.org/10.1016/j.ccb.2018.08.003> (2019).
14. Martin, P. Wound healing—aiming for perfect skin regeneration. *Science (New York, N.Y.)* **276**, 75–81 (1997).
15. Gurtner, G. C., Werner, S., Barrandon, Y. & Longaker, M. T. Wound repair and regeneration. *Nature* **453**, 314–321, <https://doi.org/10.1038/nature07039> (2008).
16. Shaw, T. J. & Martin, P. Wound repair at a glance. *Journal of cell science* **122**, 3209–3213, <https://doi.org/10.1242/jcs.031187> (2009).
17. Tsai, C. R., Wang, Y. & Galko, M. J. Crawling wounded: molecular genetic insights into wound healing from *Drosophila* larvae. *Int J Dev Biol* **62**, 479–489, <https://doi.org/10.1387/ijdb.180085mg> (2018).
18. Galko, M. J. & Krasnow, M. A. Cellular and genetic analysis of wound healing in *Drosophila* larvae. *PLoS biology* **2**, E239, <https://doi.org/10.1371/journal.pbio.0020239> (2004).
19. Wu, Y. *et al.* A blood-borne PDGF/VEGF-like ligand initiates wound-induced epidermal cell migration in *Drosophila* larvae. *Current biology: CB* **19**, 1473–1477, <https://doi.org/10.1016/j.cub.2009.07.019> (2009).
20. Tsai, C. R., Anderson, A. E., Burra, S., Jo, J. & Galko, M. J. Yorkie regulates epidermal wound healing in *Drosophila* larvae independently of cell proliferation and apoptosis. *Developmental biology* **427**, 61–71, <https://doi.org/10.1016/j.ydbio.2017.05.006> (2017).
21. Kwon, Y. C., Baek, S. H., Lee, H. & Choe, K. M. Nonmuscle myosin II localization is regulated by JNK during *Drosophila* larval wound healing. *Biochemical and biophysical research communications* **393**, 656–661, <https://doi.org/10.1016/j.bbrc.2010.02.047> (2010).
22. Baek, S. H., Kwon, Y. C., Lee, H. & Choe, K. M. Rho-family small GTPases are required for cell polarization and directional sensing in *Drosophila* wound healing. *Biochemical and biophysical research communications* **394**, 488–492, <https://doi.org/10.1016/j.bbrc.2010.02.124> (2010).
23. Lesch, C., Jo, J., Wu, Y., Fish, G. S. & Galko, M. J. A targeted UAS-RNAi screen in *Drosophila* larvae identifies wound closure genes regulating distinct cellular processes. *Genetics* **186**, 943–957, <https://doi.org/10.1534/genetics.110.121822> (2010).
24. Baek, S. H. *et al.* Requirement for Pak3 in Rac1-induced organization of actin and myosin during *Drosophila* larval wound healing. *FEBS letters* **586**, 772–777, <https://doi.org/10.1016/j.febslet.2012.01.061> (2012).
25. Longmate, W. M. & Dipersio, C. M. Integrin Regulation of Epidermal Functions in Wounds. *Adv Wound Care (New Rochelle)* **3**, 229–246, <https://doi.org/10.1089/wound.2013.0516> (2014).
26. Park, S. H. *et al.* Requirement for and polarized localization of integrin proteins during *Drosophila* wound closure. *Molecular biology of the cell* **29**, 2137–2147, <https://doi.org/10.1091/mbc.E17-11-0635> (2018).
27. Stevens, L. J. & Page-McCaw, A. A secreted MMP is required for reepithelialization during wound healing. *Molecular biology of the cell* **23**, 1068–1079, <https://doi.org/10.1091/mbc.E11-09-0745> (2012).
28. Chakrabarti, P. *et al.* A dPIP5K dependent pool of phosphatidylinositol 4,5 bisphosphate (PIP₂) is required for G-protein coupled signal transduction in *Drosophila* photoreceptors. *PLoS Genet.* **11**, e1004948, <https://doi.org/10.1371/journal.pgen.1004948> (2015).
29. Claret, S., Jouette, J., Benoit, B., Legent, K. & Guichet, A. PI(4,5)P₂ produced by the PI4P5K SKTL controls apical size by tethering PAR-3 in *Drosophila* epithelial cells. *Current biology: CB* **24**, 1071–1079, <https://doi.org/10.1016/j.cub.2014.03.056> (2014).
30. Gupta, A., Fabian, L. & Brill, J. A. Phosphatidylinositol 4,5-bisphosphate regulates cilium transition zone maturation in *Drosophila* melanogaster. *Journal of cell science* **131**, <https://doi.org/10.1242/jcs.218297> (2018).
31. Gervais, L., Claret, S., Januschke, J., Roth, S. & Guichet, A. PIP5K-dependent production of PIP₂ sustains microtubule organization to establish polarized transport in the *Drosophila* oocyte. *Development (Cambridge, England)* **135**, 3829–3838, <https://doi.org/10.1242/dev.029009> (2008).
32. Mavrakakis, M., Rikhy, R. & Lippincott-Schwartz, J. Plasma membrane polarity and compartmentalization are established before cellularization in the fly embryo. *Developmental cell* **16**, 93–104, <https://doi.org/10.1016/j.devcel.2008.11.003> (2009).
33. Hassan, B. A. *et al.* skittles, a *Drosophila* phosphatidylinositol 4-phosphate 5-kinase, is required for cell viability, germline development and bristle morphology, but not for neurotransmitter release. *Genetics* **150**, 1527–1537 (1998).
34. Tepass, U., Tanentzapf, G., Ward, R. & Fehon, R. Epithelial cell polarity and cell junctions in *Drosophila*. *Annu Rev Genet* **35**, 747–784, <https://doi.org/10.1146/annurev.genet.35.102401.091415> (2001).
35. Compagnon, J., Gervais, L., Roman, M. S., Chamot-Boeuf, S. & Guichet, A. Interplay between Rab5 and PtdIns(4,5)P₂ controls early endocytosis in the *Drosophila* germline. *Journal of cell science* **122**, 25–35, <https://doi.org/10.1242/jcs.033027> (2009).
36. Fabian, L. *et al.* Phosphatidylinositol 4,5-bisphosphate directs spermatid cell polarity and exocyst localization in *Drosophila*. *Molecular biology of the cell* **21**, 1546–1555, <https://doi.org/10.1091/mbc.E09-07-0582> (2010).
37. Park, J. *et al.* Ciliary Phosphoinositide Regulates Ciliary Protein Trafficking in *Drosophila*. *Cell Rep* **13**, 2808–2816, <https://doi.org/10.1016/j.celrep.2015.12.009> (2015).
38. Di Paolo, G. *et al.* Recruitment and regulation of phosphatidylinositol phosphate kinase type 1 gamma by the FERM domain of talin. *Nature* **420**, 85–89, <https://doi.org/10.1038/nature01147> (2002).
39. Lee, H. S. *et al.* Characterization of an actin-binding site within the talin FERM domain. *J Mol Biol* **343**, 771–784, <https://doi.org/10.1016/j.jmb.2004.08.069> (2004).
40. Tsujioka, M. *et al.* Talin couples the actomyosin cortex to the plasma membrane during rear retraction and cytokinesis. *Proceedings of the National Academy of Sciences of the United States of America* **109**, 12992–12997, <https://doi.org/10.1073/pnas.1208296109> (2012).
41. Farooqui, R. & Fenteany, G. Multiple rows of cells behind an epithelial wound edge extend cryptic lamellipodia to collectively drive cell-sheet movement. *Journal of cell science* **118**, 51–63, <https://doi.org/10.1242/jcs.01577> (2005).
42. Chen, C. *et al.* Targeting type I gamma phosphatidylinositol phosphate kinase inhibits breast cancer metastasis. *Oncogene* **34**, 4635–4646, <https://doi.org/10.1038/nc.2014.393> (2015).
43. Cao, S. *et al.* Silencing of type I gamma phosphatidylinositol phosphate kinase suppresses ovarian cancer cell proliferation, migration and invasion. *Oncol Rep* **38**, 253–262, <https://doi.org/10.3892/or.2017.5670> (2017).
44. Thapa, N., Tan, X., Choi, S., Wise, T. & Anderson, R. A. PIPKgamma and talin couple phosphoinositide and adhesion signaling to control the epithelial to mesenchymal transition. *Oncogene* **36**, 899–911, <https://doi.org/10.1038/nc.2016.267> (2017).
45. Franke, J. D., Montague, R. A. & Kiehart, D. P. Nonmuscle myosin II generates forces that transmit tension and drive contraction in multiple tissues during dorsal closure. *Current biology: CB* **15**, 2208–2221, <https://doi.org/10.1016/j.cub.2005.11.064> (2005).
46. Pearn, M. T., Randall, L. L., Shortridge, R. D., Burg, M. G. & Pak, W. L. Molecular, biochemical, and electrophysiological characterization of *Drosophila* norpA mutants. *The Journal of biological chemistry* **271**, 4937–4945 (1996).

Acknowledgements

We thank M. Galko, A. Guichet, D. Kiehart, J. Lippincott-Schwartz, M. Mavrakakis, and S. Parkhurst for providing fly stocks and antibodies, and the Bloomington Stock Center, the National Institute of Genetics in Japan, and the Vienna *Drosophila* Resource Center for fly stocks. We also thank our colleagues in the Choe lab for helpful discussions. This work was supported by the National Research Foundation of Korea (NRF) grant funded by the Korean Government, Ministry of Science and ICT (2015R1A2A2A01006660 and 2019R1F1A1044593) to K.-M.C.

Author contributions

S.H.P., C.W.L. and K.M.C. conceived the experiments. S.H.P. and C.W.L. performed the experiments. S.H.P., C.W.L. and K.M.C. analysed and processed the data. S.H.P., C.W.L. and K.M.C. wrote the manuscript.

Competing interests

The authors declare no competing interests.

Additional information

Supplementary information is available for this paper at <https://doi.org/10.1038/s41598-019-52743-z>.

Correspondence and requests for materials should be addressed to K.-M.C.

Reprints and permissions information is available at www.nature.com/reprints.

Publisher's note Springer Nature remains neutral with regard to jurisdictional claims in published maps and institutional affiliations.



Open Access This article is licensed under a Creative Commons Attribution 4.0 International License, which permits use, sharing, adaptation, distribution and reproduction in any medium or format, as long as you give appropriate credit to the original author(s) and the source, provide a link to the Creative Commons license, and indicate if changes were made. The images or other third party material in this article are included in the article's Creative Commons license, unless indicated otherwise in a credit line to the material. If material is not included in the article's Creative Commons license and your intended use is not permitted by statutory regulation or exceeds the permitted use, you will need to obtain permission directly from the copyright holder. To view a copy of this license, visit <http://creativecommons.org/licenses/by/4.0/>.

© The Author(s) 2019